Astron. Astrophys. 356, 339–346 (2000)

ASTRONOMY AND ASTROPHYSICS

Dynamical taxonomy of comets and asteroids based on the Lyapunov indicators

An analysis of the relevance of splitting

G. Tancredi[1], **V. Motta**[1,2], **and C. Froeschlé**[3]

[1] Departamento de Astronomía, Facultad de Ciencias, Iguá 4225, 11400 Montevideo, Uruguay (gonzalo@fisica.edu.uy)
[2] Instituto de Astrofísica de Canarias, E-38200 La Laguna, Tenerife, Spain (vmotta@ll.iac.es)
[3] Observatoire de Nice, BP 4229, F-06304, Nice Cedex 04, France (claude@obs-nice.fr)

Received 27 April 1998 / Accepted 26 January 2000

Abstract. By comparison of different parameters associated with a chaotic evolution, we discuss the relation between several populations of inner Solar System bodies. Tancredi (1998) found that the observed sample of Jupiter family comets (JFCs) and near-Earth asteroids (NEAs) have Lyapunov times (the inverse of Lyapunov characteristic exponents) grouped in the range between 50 and 150 yr, however the dynamical evolution is strikingly different.

By numerical integrations of the gravitational equations we compute a finite estimate of the Lyapunov characteristic exponent, the so-called Lyapunov characteristic indicators (LCIs). The LCI is found by adding short time contributions, the so-called 'local Lyapunov characteristic indicators' (Froeschlé et al. 1993). The distribution of the local Lyapunov characteristic indicators (DLI) is invariant within a chaotic region and gives us more complete information about the chaotic behaviour.

To compare the DLIs of different objects we compute the first four moments of the distributions. Though JFCs and NEAs have similar LCIs, the analysis of the four moments makes possible the distinction between the two populations, since they occupy separate regions in the moment phase-space.

We discuss the origin of the Jupiter family as the result of the splitting of a giant comet several thousand years ago. We simulate that event and integrate the dynamical evolution of the fragments. By comparing the DLIs of the fragments with the present JF objects, we observe a much more compact distribution of moments in the simulations than in the real population. The splitting hypothesis is not a plausible explanation for the origin of JFCs. Neither is there evidence for a few-body splitting event generating ~ 10 comets. Nevertheless, the comparison of DLIs proves to be a useful tool for discussing some splitting events already suggested among observed JFCs.

Key words: chaos – celestial mechanics, stellar dynamics – comets: general – minor planets, asteroids

1. Introduction

Comets are generally classified into three dynamical groups: long-period ($P > 200$ yr), intermediate-period or Halley-type (20 yr $< P < 200$ yr) and short-period ($P < 20$ yr). Among the short-period comets we define the Jupiter family (hereafter JF) as those comets with $P < 20$ yr, perihelion distance inside Jupiter's orbit ($q < 5.2$ AU) and Tisserand's parameter (T) with respect to the planet between 2 and 3 approximately.

The dynamics of JF comets (JFCs) is chaotic due to close encounters with the planet, and divergence of neighbouring orbits is often seen on time scales of several decades (Tancredi 1994). This chaoticity can be estimated by the Lyapunov characteristic exponents.

On the other hand, near-Earth asteroids (NEAs) are objects that approach the Earth's orbit ($q < 1.5$ AU) and are known to be chaotic with a Lyapunov characteristic exponent similar to the JFCs (Tancredi 1998). The fact that some NEAs are found in orbits similar to cometary orbits, led to the idea that some NEAs could be dead JFCs.

One of the objectives of this paper is to test this hypothesis. In order to do this, we compare different parameters associated with the chaotic evolution of the JFCs and NEAs. We include in the comparison Halley-type comets and the first ten numbered asteroids (main belt) as a test population.

Several hypothesis have been proposed for the origin of the JFCs. Although it is largely accepted that most JFCs originated in the trans-Neptunian belt, the relative contribution of the different sources to the present population is stil under discussion. One of the hypotheses suggests that a giant comet could have split to generate the present population (Clube & Napier 1986). We investigate this assumption using parent comets with different Tisserand constants. Furthermore, we analyse the relevance of small splitting events by looking for clusters inside the JF.

The outline of this paper is as follows. In Sect. 2 we present the theoretical background. In Sect. 3 we compare the different population of objects. In Sect. 4 we describe a method to find clusters among a population of objects. In Sect. 5 we work with random samples to search for groups inside the JF. In Sect. 6 we

analyse the possibility of a cometary splitting. And in Sect. 7 we derive our conclusions.

2. Theoretical model

2.1. The Lyapunov characteristic exponent

It is known that nearby trajectories of integrable systems diverge linearly and that the chaotic region is characterized by an exponential-like divergence of such orbits. Lyapunov characteristic exponents are a quantitative measure of the rate of exponential divergence. The maximal Lyapunov characteristic exponent (γ) is defined as

$$\gamma = \lim_{\substack{d_0 \to 0 \\ t \to \infty}} \frac{1}{t} \ln\left(\frac{d}{d_0}\right), \tag{1}$$

where d is the separation from a given orbit at time t, for an initial separation d_0.

To compute γ we use the renormalization method of Benettin and Strelcyn (1978). Consider two orbits starting at P_0 and P_0'. Let d_0 be the distance between P_0 and P_0'. After a time step τ, P_0 is at P_1 and P_0' at P_1'. If $d_1 = dist(P_1, P_1')$ then we choose two new starting points P_1 and P_1'' (this one along the direction P_1P_1') such that $dist(P_1, P_1'') = d_0$ and so on. Then

$$\gamma = \lim_{\substack{d_0 \to 0 \\ n \to \infty}} \frac{1}{n\tau} \sum_i \ln\left(\frac{d_i}{d_0}\right). \tag{2}$$

By numerical integration we compute a finite estimate of the maximal Lyapunov characteristic exponent, the so-called 'Lyapunov characteristic indicator' (LCI) (Froeschlé et al. 1993) by

$$LCI(d_0, n) = \frac{1}{n\tau} \sum_i \ln\left(\frac{d_i}{d_o}\right). \tag{3}$$

The parameters inside the sum, i.e.

$$a_i(d_0, \tau) = \ln\left(\frac{d_i}{d_o}\right), \tag{4}$$

have been called the 'local indicators' (Froeschlé et al. 1993) or 'stretching numbers' (Voglis & Contopoulos 1994).

2.2. Distribution of local Lyapunov characteristic indicators

The distribution of the local Lyapunov characteristic indicators a (or shortly distribution of local indicators—DLI) is given by the fraction dn/n of values of a in the interval $(a, a + da)$ after a large number of renormalization steps, n, divided by da:

$$S(a) = \frac{dn}{n\, da}. \tag{5}$$

(For an example of a DLI see Fig. 1.) By definition $\int_{-\infty}^{+\infty} S(a)\, da = 1$. It is easy to see that the LCI is related to the first moment of the values of a through

$$LCI = \frac{1}{n\tau} \int_{-\infty}^{+\infty} S(a)\, a\, da. \tag{6}$$

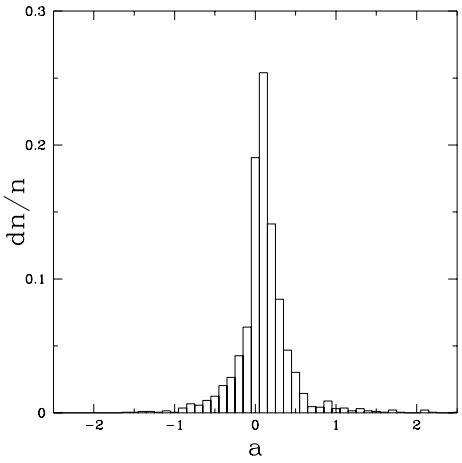

Fig. 1. Example of a distribution of local variations.

If the LCI is positive the distribution is asymmetric with respect to $a = 0$.

Voglis and Contopoulos (1994) found that the DLI ("Lyapunov spectra" in their notation) has the following characteristics:

- it is invariant along the same orbit,
- it does not depend on the initial conditions if the conditions are in the same connected chaotic domain of the phase space.

As a consequence of these results, instead of taking one orbit for many periods, one can take several orbits in the chaotic domain and superimpose its distributions. The DLI can then be computed from calculations of different orbits over short times, although this is not the procedure we use for our calculations. Besides, one can check whether the orbits belong to the same connected chaotic region.

Another relevant result is that two largely chaotic systems may have different DLIs, even if their Lyapunov characteristic exponents are equal (Contopoulos et al. 1995).

After defining the DLI, we face the problem of how to compare two of them. Following Froeschlé et al. (1993), we characterize each distribution using the first two moments (the mean, m, and the variance, σ) and the Fisher coefficients, γ_1 and γ_2, which measure respectively the asymmetry and the flatness with respect to the normal distribution:

$$m = E(a) \tag{7}$$

$$\sigma = \sqrt{E(a-m)^2} \tag{8}$$

$$\gamma_1 = \frac{\mu_3}{\sigma^3} \tag{9}$$

$$\gamma_2 = \frac{\mu_4}{\sigma^4} - 3 \tag{10}$$

where $\mu_p = E(a-m)^p$, and $E(X)$ is the expected value of X.

Hence, the DLIs are seen as points in a four-dimensional space using m, σ, γ_1, γ_2 as coordinates.

2.3. Computational model

We use numerical integration of the equations of motion for a long time span to compute the LCIs and DLIs. Our dynamical model includes the Sun (with the mass of Mercury added to the Sun) and all the planets from Venus to Neptune. The equations of motion of the massless objects, in a heliocentric frame of reference, are integrated by Everhart's (1985) $15^{\rm th}$ order RADAU integrator.

3. Integrated populations

We built the DLIs of the following groups of objects:

- 145 comets that belong to the JF
- 307 near-Earth asteroids (NEAs)
- 25 Halley-type comets
- 10 first numbered asteroids (main belt)

The starting conditions for the JF and Halley-type comets correspond to the last observed apparition taken from the $7^{\rm th}$ edition of the Catalogue of Cometary Orbits (Marsden & Williams 1992).

The set of NEAs is integrated using the starting conditions given by D. Steel (personal communication). Finally, the initial conditions for the 10 first numbered asteroids are taken from the 'Ephemerides of Minor Planets for 1995' (Institute of Theoretical Astronomy, Russian Academy of Science).

All these objects were integrated separately into the dynamical model described above for $20\,000$ yr with a renormalization time step of 5 years.

The JF comets are integrated for a period of $20\,000$ yr unless they are ejected from the Jupiter family as defined above, i.e. the integration stops if q gets larger than 5.2 AU or the period gets larger than 20 yr. If the integration lasts less than $15\,000$ yr, the object is disregarded. We end up with 123 of the 145 original comets with integrations lasting for more than $15\,000$ yr.

Fig. 2 shows the moments of the DLI for the different populations projected over different combinations of axes. Note that some groups occupy separate regions in the 4D phase space although they have similar LCIs (similar m). This is the case for the NEAs and the JFCs. Fig. 2 a shows that both populations have similar m (similar LCI), but the computation of σ allow us to distinguish between them. JFCs tend to have larger σ than NEAs. This behaviour could be explained by taking into account the fact that there is a remarkable difference between the dynamical evolution of the JFCs and the NEAs. JFCs show an erratic change in their orbital elements with frequent large jumps, whereas NEAs show smooth variations. The jumps in the JF population are associated with close encounters with Jupiter. On the other hand NEAs approach the inner planets, but those encounters are not so strong. Nevertheless, the frequency of encounters is of the same order and similar to the Lyapunov time (Tancredi 1998). The Lyapunov time is then a measure of the frequency of the perturbation of the orbit. The standard deviation (σ) of the DLI measures the strength of the perturbations, i.e. stronger perturbations would lead to large absolute values of the local indicators, a, and hence large standard deviations.

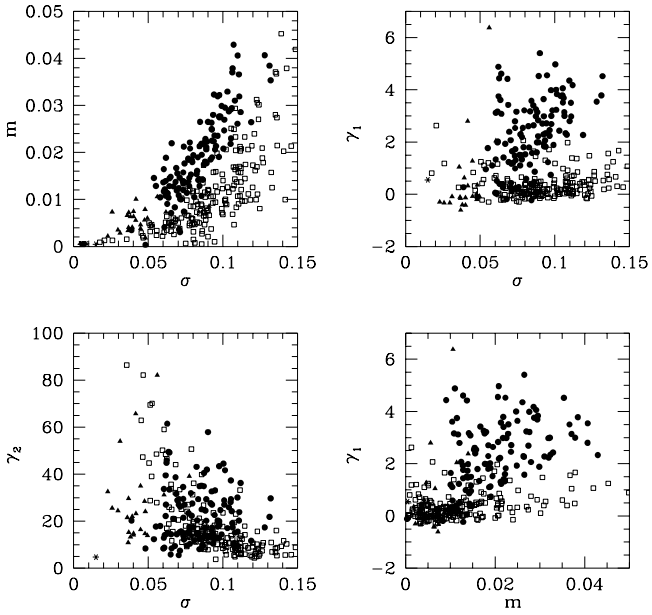

Fig. 2. Projection of the DLI distribution over different combinations of axes, where *circles* represent the Jupiter family comets, *open squares* - NEAs, *triangles* - Halley-type comets, and *stars* * the 10 first numbered (main belt) asteroids.

The large γ_1 values for JFCs compared to NEAs can also be understood in the same framework; the large values of a produce less symmetric distributions.

Regarding the other two populations of objects presented in Fig. 2, Halley-type comets have lower m and σ than JF comets. Compare to NEAs, Halley-type comets show some overlapping in the values of m, but lower values of σ. The first ten numbered main belt asteroids have the lowest values of m and σ among the studied populations.

The DLI and in particular its moments are then a useful tool to distinguish separate regions of the phase space with different dynamical behaviour though they may have similar LCIs.

In view of the small overlap between the moments of JFCs and NEAs (particularly in the (m, σ) and (m, γ_1) planes), we conclude that the contribution of JFCs to the NEA population should be small.

4. Hierarchical clustering

As we mentioned above, if two objects belong to a common region of the phase space, the DLIs should be the same; if the DLIs are calculated based on a finite time integration the estimates of the moments of the distribution should be similar. Two or more objects with similar starting conditions may have different dynamical evolutions but their DLIs in the long run should look the same. The distance in the phase space of the moments of the DLIs should be small among the members of a common group. We use a hierarchical clustering method to analyse the closeness in phase space among the members of a certain population.

We compute the distances between the DLIs (in the space with coordinates m, σ, γ_1, γ_2) of all the pairs of objects and then look for clusters. The distance between a pair of objects is defined as:

$$d = \left(\frac{(m_2 - m_1)^2}{\sigma_m} + \frac{(\sigma_2 - \sigma_1)^2}{\sigma_\sigma} + \frac{(\gamma_{1_2} - \gamma_{1_1})^2}{\sigma_{\gamma_1}} + \frac{(\gamma_{2_2} - \gamma_{2_1})^2}{\sigma_{\gamma_2}} \right)^{1/2} \quad (11)$$

where σ_m, σ_σ, σ_{γ_1} and σ_{γ_2} are the standard deviations in the values of m, σ, γ_1 and γ_2, respectively, among the members of the population.

The 'hierarchical clustering' is done following the next four steps (Zappalá et al. 1990):

1) identify the two closest objects (say j and k)
2) agglomerate them, i.e. replace the objects j and k with a new object $j\&k$
3) update all the distances, according to the following rule: the distance between $j\&k$ and any other object i is defined as the minimum distance of (i, j) and (i, k)
4) return to step **1)**

For a given distance level, the objects that agglomerate following the previous rules constitute a "cluster".

The stalactite diagram shown in Fig. 3 is built as follows. Starting from the top of the diagram, we create a black rectangle of fixed height and a width proportional to the number of members in the cluster in the highest distance level (e.g level 0.8 in Fig. 3). Each cluster is identified by a progenitor, which is defined as the cluster member with the lowest identification number.

We then proceed to the next smallest distance level. We now create rectangles as in the previous level, i.e. of the same height and width proportional to the number of members in each cluster. The new clusters are subgroups of one of the clusters of the previous level. These subclusters hang from the corresponding higher cluster. Different colours are assigned to clusters with different progenitors. Two clusters of a given level with different colours, but hanging from a cluster of the same colour, have different progenitors but a common progenitor of the progenitors, i.e. they have different fathers but a common grandfather.

The process is repeated until we reach the lowest distance level. The deepest stalactites correspond to the nearest objects in the phase space.

The highest distance level is defined at an arbitrary value where most of the objects belong to few clusters. The lowest level is chosen in such a way that there are very few pairs of members closer than the adopted value. For the examples presented in this paper, we look at the distribution of all the mutual distances between pair of members, the highest distance level is chosen at the value corresponding to the lowermost $5\,\%$ of the distribution, and the lowest level to the lowermost $0.5\,\%$.

At the top of the figure we mark the Minor Planet Centre number of the comets; e.g. for numbered comets with more than one perihelion passage we use its number; for example, number 3 for 3D/Biela; for comets with a single passage we have two cases: i) if the passage has occurred in this century we use two digits plus a letter and another digit; for example, 83C1 for 1983C1 P/Bowell-Skiff; ii) if the passage has happened in previous centuries we use three digits plus a letter and another digit; for example, 892T1 for 1892T1 D/Barnard-3.

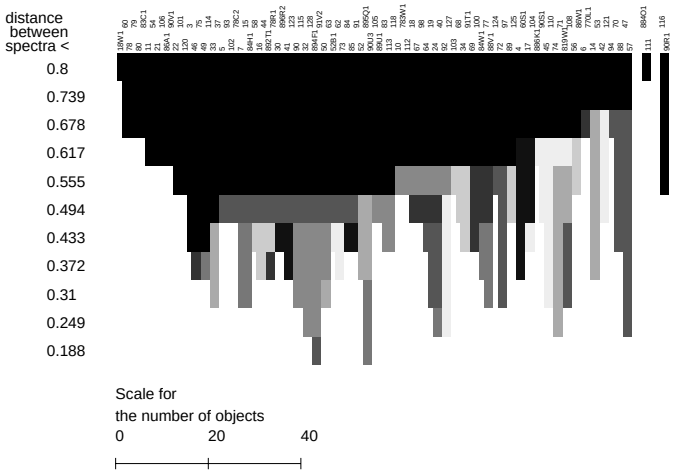

Fig. 3. Stalactite diagram for the Jupiter family comets. (See the text for an explanation of the numbers at the top of the figure.)

Fig. 3 shows that most JF comets belong to a common large cluster and that there are very few objects outside it; we cannot identify 2 or 3 different large groups. Even down to a distance of ~ 0.55, almost half of the members of the large cluster remain together. Fine structures with many subclusters are mainly created below a distance of ~ 0.6.

Most JF comets share a large common region in the 4D moment phase space denoting a similar chaotic behaviour.

The appearance of clusters of a given size at a certain distance level is a measure of the clustering grade of a population. Let us make a note of some values: clusters of ~ 50 members appear down to a distance of 0.55, of 8–10 members down to 0.43 and of 5 members down to 0.31. At distances below 0.31 there are 13 clusters of two or more members.

A clustering pattern has little significance in itself unless it is compared with other populations. Fig. 3 and the numbers just given will be used in the following sections when we compare the real JF population with some fictitious population that share the same region in 4D phase space. From these comparisons we will able to realize the significance of the clustering pattern of the JF population.

5. Few-body splitting events

After the splitting of P/Shoemaker-Levy 9 (SL9) caused by tidal forces during a close approach to Jupiter, the frequency and relevance of these events among members of the JF have been re-evaluated. Two kind of splits can be distinguished: a fragmentation of a piece of nucleus followed by a rapid increase in brightness that later disappear without important change in

the nuclear size; and a 'mitosis' type of split where more than two nuclei are formed and persist for several revolutions.

We have to bear in mind that SL9 split during a temporary satellite capture by Jupiter and later impacted the planet, but we are interested in the cases where the fragments survive into heliocentric orbits.

The cases of 42P/Neujmin 3 and 53P/Van Biesbroeck seem to be the best examples of the mitosis type of splitting. Numerical integrations show that the orbits of these two objects, previous to a very close encounter with Jupiter in 1850, were almost identical (Carusi et al. 1985). If the mitosis type of split is a frequent event it could contribute greatly to increasing the number of JFCs.

To investigate the relevance of these phenomena among the JF population we compare the small-size cluster in the sample of observed comets with a sample of points randomly distributed in the moment phase space. We focus our attention on SL9-like splitting, where ~ 10 fragment are formed. Nevertheless our analysis is not restricted to splits caused by Jupiter's tidal force, we do not make any assumption about a particular splitting mechanism.

It is very difficult to define a random sample because we do not know a priori the borders of the region in the 4D space occupied by the whole population of the JF. Taking this into account and assuming the present population as a representative sample of the whole family, the random samples are picked in the following way:

1. Enclose the distribution of the JFCs in the 4D phase space with some simple hypervolume (e.g. we set walls at the lowest and uppermost values of each moment).
2. Take a random distribution of points inside this volume.
3. Compute the distance between the new object and all the JFCs. We select 123 objects with minimum distance to any JFCs less than a given value (e.g. the median of the distribution of all the minimum mutual distance among JFCs).

By this method we ensure that the new population shares approximately the same hypervolume as the JFCs.

After that, we compute the distance between each simulated comet and built the stalactite diagram (Fig. 4).

We compare the distance level in the JF and random stalactite diagram where clusters of 8–10 members start to be formed (Figs. 3 and 4). Such kinds of clusters are formed at distances of ~ 0.4 in both samples. We then conclude that middle-size agglomerations are irrelevant in comparison with the background random distribution. There is no evidence for a large splitting event in the last few thousand years. Looking at splits leading to 2–3 nuclei, we observe that the numbers of such kinds of clusters down to a distance of 0.3 in the JF population and the random sample are similar (13 in the first one and 16 in the latter). We cannot decide whether the JF clusters are real or are just a matter of chance.

We conclude that the clustering pattern shown by the JF is indistinguishable from a random sample of points occupying the same region in the 4D phase space of moments of the DLI.

Nevertheless, to stress the usefulness of the moments of the DLI in identifying split objects, let us consider in detail the case of 42P/Neujmin 3 and 53P/Van Biesbroeck. Though we are able to reproduce in our background integration a common encounter with Jupiter in 1850 and a similar pre-encounter orbit, the orbital elements in the rest of the $20\,000$ years are remarkably different. 42P/Neujmin 3 and 53P/Van Biesbroeck occupy a rather empty region in the moment phase space, on the edge of the main cluster (for 42P/Neujmin 3: $m = 0.013$, $\sigma = 0.064$, $\gamma_1 = 4.6$, $\gamma_2 = 49$; for 53P/Van Biesbroeck: $m = 0.010$, $\sigma = 0.061$, $\gamma_1 = 3.6$, $\gamma_2 = 50$, see Fig. 2). Ordering the distance between each of these two comets and the rest of the JFCs, we found that their mutual distance, though quite large ($d = 0.80$), is the second smallest for 53P/Van Biesbroeck and the third smallest for 42P/Neujmin 3. The only object with a smaller distance to both of them is 14P/Wolf. 14P/Wolf and 53P/Van Biesbroeck are displayed as a cluster in the stalactite diagram for the JF (look at numbers 14 and 53 at the top of Fig. 3); while 42P/Neujmin 3 forms a cluster with 121P/Shoemaker-Holt 2. These two clusters are joined together at a level of 0.74; but, at this level, other objects also join the cluster. They finally form a long "string" in the 4D phase space that, at this level, is connected with the background large cluster. This example indicates a drawback of the clustering criteria we have chosen (in particular step 3 of the hierarchical clustering algorithm); i.e. the method tends to favor long "strings" with objects that are very separated at the ends in comparison with groups of objects rather separated from the rest.

It is beyond the scope of this paper to investigate the possible physical connection between the progenitor of 42P/Neujmin 3 and 53P/Van Biesbroeck with 14P/Wolf and/or 121P/Shoemaker-Holt 2; we simply mention that 14P/Wolf suffered two very close encounters after 1850 and 121P/Shoemaker-Holt 2 made a full loop around Jupiter in 1981 which makes it very difficult to predict their orbits reliably at the time of the splitting. We conclude that, though the elements of the two split comets differ during most of the integrations possibly due to the lack of precision involved in the numerical integrations of chaotic orbits, the closeness between the DLIs reinforce the hypothesis of a common origin (and hence a common chaotic region) for the two objects.

6. The splitting of a giant comet

The flux of comets coming from the Oort cloud and ending in JF orbits has been shown to be very small (Duncan et al. 1988; Rickman 1991). Furthermore, the fact that JF comets move in direct orbits with low inclinations led Fernández (1980) to speculate that most of these objects come from a trans-Neptunian belt. This trans-Neptunian cometary disc has been named the Edgeworth–Kuiper belt. By numerical modelling the process of hanging down comets from the Edgeworth–Kuiper belt to the JF, Duncan et al. (1988) and lately Levison & Duncan (1997) showed that objects coming from this putative source are able to explain the distribution of the observed population. In the mean time several other alternative sources have been proposed

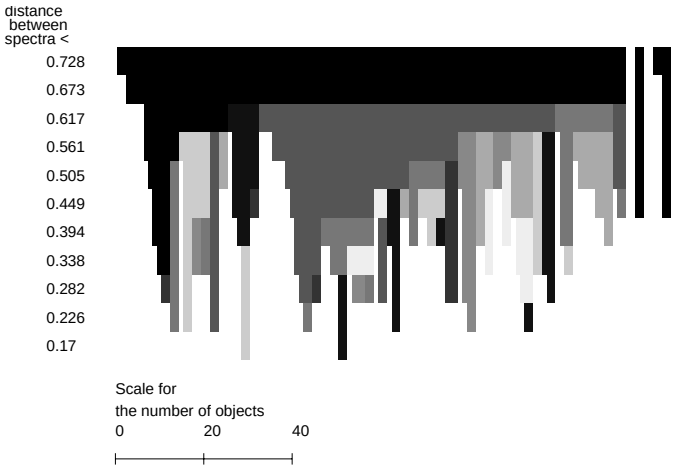

Fig. 4. Stalactite diagram for the random samples of comets.

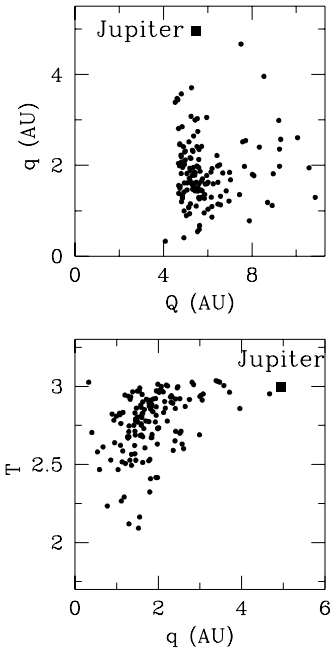

Fig. 5a and b. Distribution of the Jupiter family comets in the **a** (Q, q) plane; and **b** in the (q, T) plane.

to explain the origin of JF comets; e.g. an extended inner core of the Oort cloud (Bailey 1992) or the existence of a single large progenitor that might be broken into ordinary comets several thousand years ago (Clube & Napier 1986).

Although after the discovery of more than 100 trans-Neptunian objects it is largely accepted than most JF comets come from the Edgeworth–Kuiper belt, the relative contribution of other sources is still an open problem. If a large-scale comet splitting events have occurred in the past the required flux from other distant reservoirs could be lower. Our goal is to determine whether the pieces of a split comet maintain a certain memory in our 4D space. If the pieces show this behaviour we are able to compare them to the observed JF.

Table 1.

Orbital element	T=2.9	T=2.8	T=2.6
q (AU)	3.78	1.50	0.50
e	0.26	0.5	0.83
i (deg)	10.0	10.0	10.0
ω (deg)	0.0	0.0	0.0
Ω (deg)	10.0	10.0	10.0
M_o	0.0	0.0	0.0

6.1. Initial conditions

The hypothesis of the splitting of a comet is studied in a way similar to that described by Pittich & Rickman (1994). We choose the orbits of a few fictitious parent comets such that their perihelion distances are inside Jupiter's orbit ($q < 5.2$ AU) and their Tisserand parameter between 2.5 and 3. This set of values corresponds to a typical JF orbit as is shown in the distribution in the (Q, q) and (q, T) planes of the JF comets presented in Fig. 5 a and b, respectively (Q–aphelion distance). From each progenitor we create a set of splitting fragments as described below.

There are three parent comets under consideration. They differ in their Tisserand parameter (T) values and in the eccentricities of their orbits. One of the parents has a low value of T (2.6) and high eccentricity (0.83), the other one has a moderately high value of T (2.8) and an intermediate eccentricity (0.5), while the last one has a high value of T (2.9) and low eccentricity (0.26) (the orbital elements of the parents are presented in Table I). All of them have moderately low inclinations, typical of JF comets.

Following Pittich & Rickman (1994), we assume that the progenitors may split at any point in their orbits. Therefore we have taken twelve splitting events for each progenitor, uniformly separated in time by $1/12$ of the orbital period. Each of these events was modelled by starting seven fragments with slightly different velocities. One of the fragments has the same velocity as the parent comet, and the other six receive velocity increments of $\pm 5 \times 10^{-7}$ AU per day and $\pm 10^{-6}$ AU per day along one of the x, y or z axes. We get a set of 144 fragments for each progenitor. This number of fragments is chosen to be close to the number of known JFCs (145).

6.2. Orbital integration

The dynamical model and the integration algorithm is the same as before (Sect. 2.3). The integration is done over $10\,000$ years.

In Fig. 6 we show several snapshots in the (Q, q) plane of the set of objects whose parent has $T = 2.9$. At $t = 4\,000$ years most of the objects escape from the plotted (Q, q) domain. Comparing this result with the distribution of the JF in the (Q, q) plane (Fig. 5 a), we conclude that these fragments do not represent the real JF.

In Figs. 7 and 8 we present snapshots in the (q, T) domain for the set of objects with $T = 2.6$ and $T = 2.8$. Both sets of fragments show at a different stage of the evolution a distri-

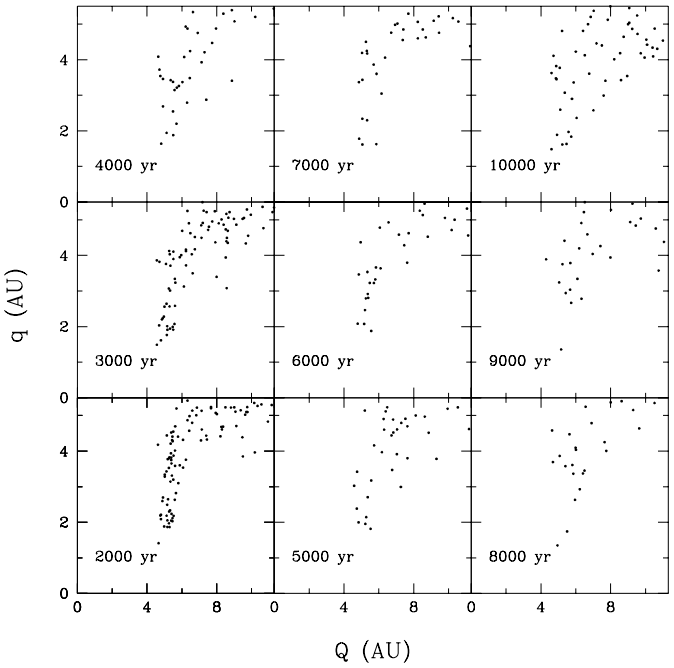

Fig. 6. Snapshots of the orbital element evolution for the fragments of parent comets with $T = 2.9$.

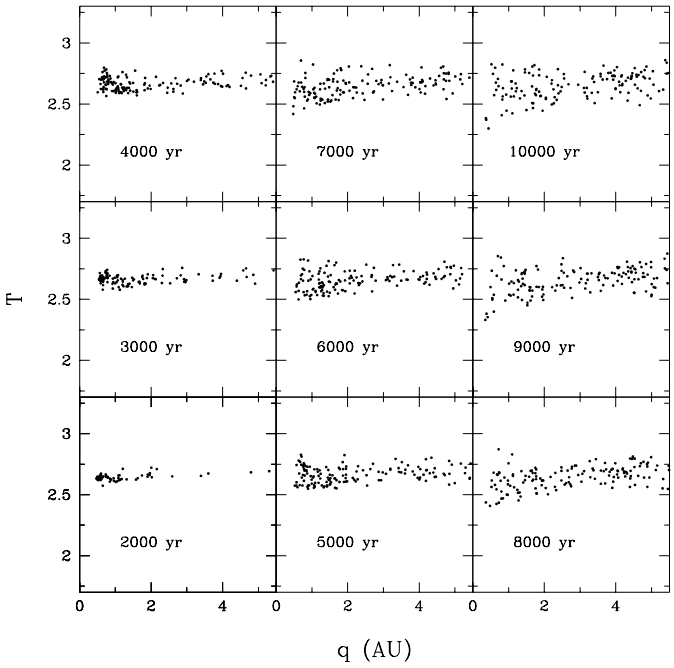

Fig. 7. Snapshots of the orbital element evolution for the fragments of parent comets with $T = 2.6$.

bution in the (q, T) plane that resembles that of the JF (Fig. 5 b). A statistical comparison between the snapshots and the JF was performed by applying the 2-dimensional Kolmogorov–Smirnov test (Press et al. 1992). For each snapshot and each progenitor we compute the distance between the (q, T) distribution and that of the JF (see Press et al. 1992 for a definition of the distance between two distributions). While for $T = 2.6$ and $T = 2.8$ a minimum distance of 0.49 was attained at some stage of the evolution, for $T = 2.9$ the distance never reached values lower than 0.72. In view of the differences in the (Q, q) and (q, T) domains between the JF and the $T = 2.9$ snapshots we decide to exclude the latter in the following analysis.

The stalactite diagram was applied to the set of objects corresponding to $T = 2.6$ and $T = 2.8$ and the results are shown in the Figs. 9 and 10, respectively. To compute the mutual distance between a pair of objects we use Eq. (11) but normalized by the standard deviation $(\sigma_m, \sigma_\sigma, \sigma_{\gamma_1}, \sigma_{\gamma_2})$ of the JF in order to have a similar distance scale.

Comparing the distance levels for the pieces of the simulated comets (Figs. 9 and 10) with that of the real JFCs (Fig. 3), we can see that large clusters are formed at different distance levels. While in the JF a very large cluster with more than 50 members appears at a distance level of ~ 0.55, in the split comets with $T = 2.6$ and $T = 2.8$ this happens at ~ 0.41.

Thus, although the pieces of the parent comet escape from their original positions in the element space, and after a few thousand years the distribution in the (q, T) plane resembles the JF, the splitting comets maintain a certain memory in the moment phase space that would allow us to identify them as a compact cluster after several thousand years. This conclusion is in contradiction with the statement by Pittich and Rickman:

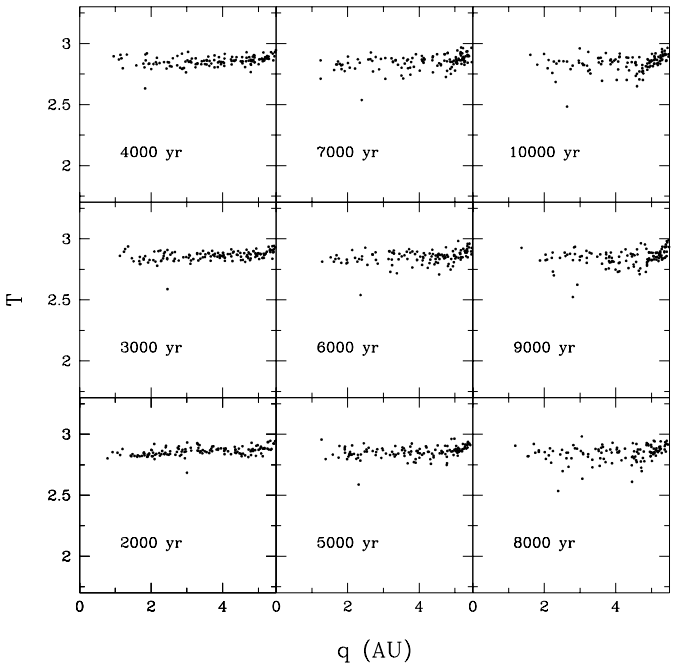

Fig. 8. Snapshots of the orbital element evolution for the fragments of parent comets with $T = 2.8$.

"the sets of fragments lose their memory of a common origin very rapidly." This is true for the orbital elements but not for the moments of the distribution of local indicators. This indicates that the JFCs could not be the product of the splitting of a giant comet during the last $\sim 10\,000$ years.

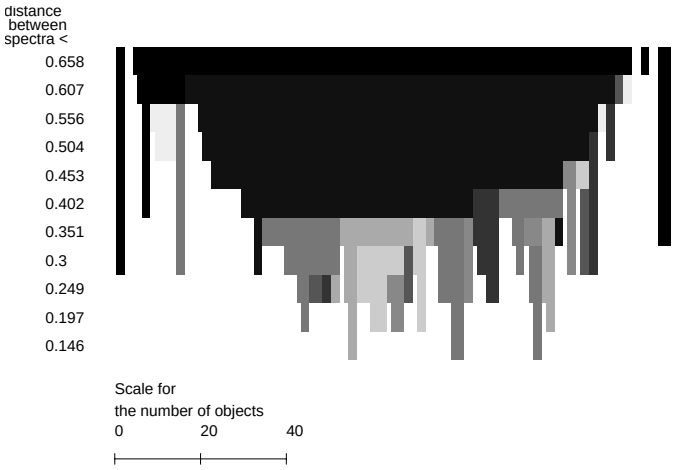

Fig. 9. Stalactite diagram for the family produced by the splitting of a comet with $T = 2.6$.

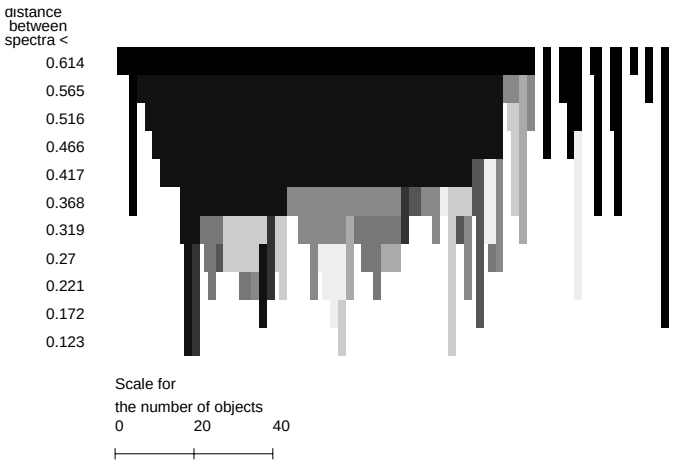

Fig. 10. Stalactite diagram for the family produced by the splitting of a comet with $T = 2.8$.

7. Conclusions

Lyapunov characteristic indicators (LCIs) are a useful tool for characterizing the chaotic behaviour of an orbit but it is rather poor when we are interested in the cause of the chaoticity.

We have found two populations of solar system objects (JFCs and NEAs) with similar LCI but strikingly different dynamical behaviour. The distribution of local indicators (DLIs) and in particular its first moments, give us much information that makes the distinction between the two populations possible.

The differences are understood as a consequence of the kind of evolution: while JFCs suffer strong perturbations by Jupiter during the encounters, the NEAs have mild perturbations by the inner planets. Since the frequencies of relevant encounters are similar, the mean of the DLI, and hence the LCI, is of the same order (Tancredi 1998); but the broadness (σ) and asymmetry (γ_1) of the DLI are generally larger for JFCs than for NEAs.

There is no evidence for a splitting event generating ~ 10 JFCs; the distances at which these kinds of clusters are formed is comparable to the distance of such clusters in a fictitious population with moments randomly distributed in the 4D hypervolume occupied by JFCs.

The usefulness of the moments of DLIs in discussing the dynamical connection between objects is shown in the case of the possible common origin of 42P/Neujmin 3 and 53P/Van Biesbroeck. Although the orbits are very different in the $20\,000$ years integration, the moments of DLIs are relatively close and far apart from the rest of JFCs. This result reinforces the hypothesis proposed by Carusi et al. (1985) that 42P/Neujmin 3 and 53P/Van Biesbroeck originated from a splitting event that occurred during a very close encounter with Jupiter in 1850.

We also analyse the hypothesis of the origin of the JF by the splitting of a giant comet a few thousand years ago. We conclude that in order to reproduce the actual distribution of objects in the $q-Q$ and $q-T$ planes, a parent body is required with a moderate value of the Tisserand parameter (T$\simeq 2.6 - 2.8$). But a trace of the common origin should still be present in the distribution of moments of DLIs as a highly compact distribution with large clusters of several tens of members forming at shorter mutual distances than in the observed JF. A single giant comet splitting is not then a plausible proposal for the origin of an important part of the present JFCs.

References

Bailey M.E., 1992, Cel. Mec. and Dyn. Astron. 54, 49
Benettin G., Strelcyn J.M., 1978, Phys. Rev. 17, 773
Carusi A., Kresák L. Perrozzi E., Valsecchi G.B., 1985, In: Carusi A., Valsecchi G.B. (eds.) Dynamics of Comets: Their Origin and Evolution. D. Reidel Publishing Company, p. 319
Clube S.V.M., Napier W.M., 1986, In: Smoluchowski R., Bahcall J.N., Matthews M.S. (eds.) The Galaxy and the Solar System. Univ. Arizona Press, p. 260
Contopoulos G., Voglis N., Efthymiopoulos C., Grousousakou R., 1995, Hunter J., Wilson R. (eds.) Waves in Astrophysics
Duncan M., Quinn T., Tremaine S., 1988, ApJ 328, L69
Everhart E., 1985, In: Carusi A., Valsecchi G.B. (eds.) Dynamics of Comets: Their Origin and Evolution. D. Reidel Publishing Company
Fernández J.A., 1980, MNRAS 192, 481
Froeschlé C., Froeschlé Ch., Lohinger E., 1993, Celestial Mechanics and Dynamical Astronomy. Kluwer Academic Publishers, p. 56, 307
Levison H., Duncan M., 1997, Icarus 127, 13
Marsden B.G., Williams G.V., 1992, Catalogue of Cometary Orbits, 7^{th} Edition, Minor Planet Centre, Smithsonian Astrophys. Obs.
Pittich E., Rickman H., 1994, A&A 281, 579
Press W., Teukolsky S., Vetterling W., Flannery B., 1992, Numerical Recipes in Fortran. Cambridge Univ. Press
Rickman H., 1991, In: Benest D., Froeschlé C. (eds.) Interrelations Between Physics and Dynamics for Minor Bodies in the Solar System. Edition Frontières, Gif-sur-Yvette, p. 107
Tancredi G., 1994, A&A 299, 288
Tancredi G., 1998, Celestial Mechanics 70, 181
Voglis N., Contopoulos G., 1994, J. Phys. A 26, 4899
Zappalá V., Cellino A., Farinella P., Knežević Z., 1990, AJ 100, 2030